Focal therapy of neuroblastoma using silk films to deliver kinase and chemotherapeutic agents *in vivo*

F. Philipp Seib[a], Jeannine Coburn[b], Ilona Konrad[b], Nikolai Klebanov[b], Gregory T. Jones[c], Brian Blackwood[d], Alain Charest[e], David L. Kaplan[b], and Bill Chiu[6f*]

(a) Strathclyde Institute of Pharmacy and Biomedical Sciences, University of Strathclyde, Glasgow, UK
(b) Department of Biomedical Engineering, Tufts University, Medford, MA, USA
(c) Department of Biochemistry, Tufts University, Medford, MA, USA
(d) Department of Surgery, Rush University Medical Center, Chicago, IL USA
(e) Department of Neurosurgery, Tufts Medical Center, Boston, MA, USA
(f) Department of Surgery, University of Illinois at Chicago, Chicago, IL, USA

Keywords: neuroblastoma, chemotherapy, controlled release, silk

Corresponding Author:
[*]Bill Chiu, MD
Department of Surgery
University of Illinois at Chicago
840 S. Wood Street, Suite 416
Chicago, IL 60612
USA

Phone: 312-413-7707
Fax: 312-355-1497
E-mail: bchiumd@uic.edu

ABSTRACT

Current methods for treatment of high-risk neuroblastoma patients include surgical intervention, in addition to systemic chemotherapy. However, only limited therapeutic tools are available to pediatric surgeons involved in neuroblastoma care, so the development of interoperative treatment modalities is highly desirable. This study presents a silk film library generated for focal therapy of neuroblastoma; these films were loaded with either the chemotherapeutic agent doxorubicin or the targeted drug crizotinib. Drug release kinetics from the silk films were fine-tuned by changing the amount and physical crosslinking of silk; doxorubicin loaded films were further refined by applying a gold nanocoating. Doxorubicin-loaded, physically crosslinked silk films showed the best *in vitro* activity and superior *in vivo* activity in orthotopic neuroblastoma studies when compared to the doxorubicin-equivalent dose administered intravenously. Silk films were also suitable for delivery of the targeted drug crizotinib, as crizotinib-loaded silk films showed an extended release profile and an improved response both *in vitro* and *in vivo* when compared to freely diffusible crizotinib. These findings, when combined with prior *in vivo* data on silk, support a viable future for silk-based anticancer drug delivery systems.

1. INTRODUCTION

Neuroblastoma is the most common extracranial tumor in childhood, with a variable disease progression ranging from complete spontaneous remission to life-threatening progression despite intensive combination therapy [1]. High-risk patients are identified using markers such as age, stage, histology, N-myc proto-oncogene status, and DNA ploidy. Although cure rates for early stage neuroblastoma are excellent, the 5-year event-free survival rate for high-risk patients remains only 40 % [2].

Current treatment options for high-risk neuroblastoma include intensive systemic neoadjuvant chemotherapy and immune modulation, followed by surgical resection [1]. Nevertheless, even after high dose chemotherapy, an abdominal tumor will still frequently extend along vital vasculatures. Pediatric surgeons are often called upon to skeletonize vessels such as the superior mesenteric artery, the celiac artery, renal vessels, or the inferior vena cava in order to excise these tumors. This is not only a treacherous and time-consuming endeavor, but the morbidity of the procedure is high and can induce vessel thrombosis, stricture, or even organ loss [3]. Furthermore, the side effects of high dose chemotherapeutic agents—including ototoxicity, myelosuppression, and nephrotoxicity—can have lasting consequences in the pediatric population [1].

Neuroblastoma cells often develop drug resistance; therefore, the development of other strategies (e.g., tumor differentiation with retinoids or immunotherapy with disialoganglioside GD2 antibodies combined with cytokines) is encouraging [1]. Kinase inhibitors that target anaplastic lymphoma kinase (ALK) have been developed for other cancers and are currently being

evaluated for use in neuroblastoma patients through the Pediatric Preclinical Testing Program of the National Cancer Institute [4]. ALK is associated with a major neuroblastoma predisposition that is reflected by somatic mutations or gene amplifications in 15 % of patients [2, 4]. Because ALK expression is largely restricted to neurons, with a strong up-regulation in neuroblastomas [5, 6], ALK inhibitors such as crizotinib are poised to have a significant impact on neuroblastoma therapy [2, 4].

Follow-up studies have demonstrated a probability of local progression of 50 % in unresected patients versus 10 % in stage 4 patients undergoing gross total resection, with an overall survival of 50 % and 11 %, respectively [7]. Thus, local-regional control of the disease appears to be a key driver for improved clinical outcome. Because high-risk neuroblastoma patients commonly undergo surgical intervention as part of their treatment, focal drug therapy at the time of surgery might be a beneficial approach for the local treatment of unresectable tumors, thereby further improving clinical outcomes.

A leaky blood vasculature and reduced lymphatic drainage are hallmarks of established solid tumors [8]. Tumor pathology has been exploited for the rational design of many intravenously administered anticancer nanomedicines (e.g., nanoparticles, micelles, liposomes) [9]; two studies have recently developed crizotinib-based nanomedicines [10, 11]. However, poor tumor perfusion and high interstitial pressure can limit nanomedicine accumulation [12]. Furthermore, intravenously administered anticancer nanomedicines cannot be administered to neuroblastoma patients undergoing surgery because tumor resection typically removes the tumor vasculature

and therefore eliminates the gateway of nanomedicines to its target site. Therefore focal therapy appears to be a better approach to treat neuroblastoma patients undergoing surgical intervention.

Focal therapy has remained largely unexplored in the neuroblastoma setting; however, clinical examples exist for other tumors, including brachytherapy of early stage breast cancer [13] and the treatment of high-grade malignant glioma and recurrent glioblastoma multiforme post-resection using controlled-release polymeric wafers to deliver carmustine (Gliadel wafers) [14, 15]. For neuroblastoma, features of an ideal drug delivery system for focal therapy would include: (i) a flexible delivery platform for different drugs; (ii) tunable drug release kinetics; (iii) biocompatibility; (iv) biodegradability; (v) conformity to the tumor/tumor bed; and (vi) unidirectional drug release toward the tumor/tumor bed.

Silk has been used in human medicine for hundreds of years as a suture material and is approved as a surgical mesh (Allergan Inc., Irvine, CA, USA). Its unique mechanical properties [16, 17], biocompatibility, and the versatility of its various formats [16] make silk attractive for various other biomedical applications, including drug delivery [18]. For example, we have been able to generate self-assembling hydrogels [19] for breast cancer focal therapy, as well as uniform silk nanoparticles that can be used for the pH-mediated lysosomotropic delivery of a model drug, doxorubicin [20]. Silk films have excellent surface conformity [21, 22] and are therefore particularly well suited for the direct application to tumors/tumor bed; the wettability of silk also promotes tight adhesion to tissues [23]. In contrast Gliadel wafers are monolithic, solid discs with no conformity to tumor margins; a physical characteristic and design feature commonly encountered with many synthetic polymeric carrier systems [24].

The goal of the present study was to develop silk films for focal drug therapy using the clinically relevant anticancer drugs, doxorubicin and crizotinib, and to assess the drug loading, drug release, and biological responses of these films, both *in vitro* and *in vivo*.

2. MATERIALS AND METHODS

Human neuroblastoma cell lines SK-N-AS (American Type Culture Collection, Manassas, VA, USA) were maintained in Dulbecco's modified Eagle's medium supplemented with 10 % fetal bovine serum, 100 IU/ml penicillin, 100 µg/ml streptomycin, and 0.1 mM non-essential amino acids. KELLY cells (Sigma-Aldrich, St Louis, MO, USA) were maintained in RPMI 1640 supplemented with 10 %v/v fetal bovine serum, 100 IU/ml penicillin, 100 µg/ml streptomycin, and 2 mM glutamine. All cells were maintained in a humidified 5 % CO_2 atmosphere at 37°C and were trypsin-passaged at 80 % confluence.

2.1 Manufacture of drug-loaded silk films

Silk was isolated from Japanese *Bombyx mori* cocoons, as previously described [25]. Briefly, cocoons were boiled in 20 mM sodium carbonate for 30 minutes, washed with deionized water, and the degummed fibers were air-dried. The silk fibers were then dissolved in 9.3 M lithium bromide at 60°C for 4 hours and the solution was dialyzed (3.4 kDa MWCO, Piece, Rockford, IL, USA) against deionized water for 60 hours. Silk films were manufactured using 1, 2, or 4 %w/v silk solutions by casting the silk on an 11 mm × 17 mm polydimethylsiloxane (PDMS) mold and allowing the solution to air-dry overnight. The resulting water soluble films were cut into 7 mm × 11 mm rectangles. A 20 minute steam autoclaving cycle was used to induce

physical crosslinks, resulting in a stabilized silk film (i.e., water insoluble). The stabilized silk films were loaded with 50 μg doxorubicin (LC Laboratories, Woburn, MA, USA) by soaking them in a doxorubicin solution and verifying loading by measuring doxorubicin-associated fluorescence of the solution (excitation 480 nm, emission 590 nm). Similarly, stabilized silk films were loaded with crizotinib by soaking them in 450 μg crizotinib for 48 hours. Drug loading was quantified by mass spectroscopy (detailed below) by determining the difference in amounts of crizotinib in the soaking solution pre- and post-loading. Water-soluble silk films with a nominal doxorubicin loading of 50 μg for each 7 mm × 11 mm film were generated by dissolving the required amount of drug in ddH_2O and adding it to the silk. This doxorubicin silk solution was cast onto PDMS, allowed to air-dry overnight, and then cut to the desired dimensions. Soluble crizotinib films were generated in an analogous fashion, but with a nominal loading of 10 μg of drug per film. Silk films with a gold backing were generated by sputter coating 7 mm × 11 mm films with 100 nm of gold, stabilizing the films by autoclaving, and finally loading with 50 μg doxorubicin using the soaking method described above.

The swelling characteristics of stabilized silk films were determined by measuring the films in their dry and wet states after a 48 h incubation in phosphate buffered saline (PBS). Similarly, the thicknesses of the films were measured with calipers before and after incubation in PBS.

2.2 Measurement of drug release from silk films

In vitro release kinetics were determined by incubating films with 1 ml of PBS under static conditions at room temperature; at each time point, the entire volume of PBS was removed and replaced with fresh PBS to ensure sink conditions. Doxorubicin release was determined by

measuring doxorubicin-associated fluorescence (excitation 480 nm, emission 590 nm). The impact of the gold backing on directional doxorubicin release was determined by casting 2 wt% agarose in PBS into a petri dish and allowing it to cool. Just before the gel had set, silk films were added to the gel and stabilized with a custom-made polystyrene frame to facilitate the correct placement of the film. After 24 h at room temperature, a Xenogen IVIS 200 imaging system, controlled by the Living Image Software 4.2 (Caliper Life Sciences, Hopkinton, CA, USA), was used to measure doxorubicin-associated fluorescence. For *in vivo* studies, the residual amount of doxorubicin remaining in the film was determined by measuring light absorbance at 482 nm. Retrieved films were dissolved using 100 µl 9.3 M lithium bromide at 60°C for 30 to 60 minutes. The resulting solution was diluted with 900 µl PBS. Absorbance values were converted to concentrations via a standard curve made in 0.93 M lithium bromide/PBS solution.

The *in vitro* release of crizotinib was measured using high pressure liquid chromatography coupled with mass spectroscopy (LC-MS, Finnigan Surveyer LC system and Finnigan LTQ, Thermo Scientific, Waltham, MA, USA). Twenty microliters of sample or standard containing 10 µM etoposide as an internal standard were injected into a C18 analytical column (Ascentis® C18 column, 3 µm particle size, 50 mm length × 2.1 mm internal diameter, Sigma-Aldrich, St Louis, MO, USA) equilibrated with 90:10 water:acetonitrile containing 0.1 %v/v formic acid. After 1.5 minutes, a gradient was started, ramping to 10:90 water:acetonitrile containing 0.1 % formic acid over 2.7 minutes and held at high acetonitrile for 2 minutes. The quantification was performed using a selective reaction monitoring (SRM) method with the transitions of *m*/*z* 450 to 260 for crizotinib. Evaluation of the total ion chromatogram was performed for etoposide using *m/z* 606 ($M+NH_4$). The main working parameters were set as follows: ion spray voltage 5.0 kV;

capillary temperature 275°C; tube lens offset 70 V; sheath gas flow rate 60; auxiliary gas flow rate 2; and sweep gas flow rate 1.4. For fragmentation of crizotinib, the settings were as follows: normalized collision energy 48; activation 0.25; and activation time 30 ms. Typical retention times were 3 minutes and 3.5 minutes for crizotinib and etoposide, respectively. Xcalibur™ Software (Thermo Scientific) was used for data acquisition and quantification of the area under the curve (AUC) for both crizotinib and etoposide peaks. The crizotinib AUC was normalized to etoposide AUC. A standard curve for crizotinib was generated to convert the normalized AUC values to concentrations.

2.3 In vitro activity of drug-loaded silk films

The *in vitro* toxicity of doxorubicin-loaded silk films was determined by plating KELLY cells at 3×10^4 cells/cm^2 in 24 well plates with 500 µl of complete medium and allowing the cultures to recover for 24 h. Next, 2 %w/v soluble silk films, stabilized silk films, or the respective doxorubicin-loaded silk films containing 50 µg of the drug were added to the cultures. A 50 µg dose of freely diffusible doxorubicin was used as a control (i.e., no silk in the system). At the indicated time points, 50 µl of AlamaBlue (Invitrogen, Grand Island USA) was added to the culture medium, and cell viability was measured after a 4 h incubation period by monitoring fluorescence (excitation wavelength 550 nm, emission wavelength 590 nm). Next, all the medium was replaced with fresh culture medium and culturing was continued. Disease relapse was mimicked by reseeding the plates at day 6 with 3×10^4 cells/cm^2 and cell viability was monitored as described above. The only two culture conditions that were not re-seeded were the control cultures, and the soluble and stabilized silk film control cultures because these had become confluent by this time point. The biological activity of crizotinib-loaded films was

assessed in a protocol analogous to that used for the doxorubicin, again using KELLY (MYCN amplified, ALK mutation) and SK-N-AS (non-MYCN amplified, no ALK mutation) cells. Stabilized silk films had a nominal crizotinib loading of 160 μg. Soluble films contained 10 μg crizotinib, while a 10 μg dose of freely diffusible crizotinib was used as a control (i.e., no silk in the system). Cell viability was determined by a protocol analogous to that used in the doxorubicin studies detailed above. The IC_{50} values for crizotinib and doxorubicin were determined by plating cells at a density of 3×10^4 cells/cm^2 and the cells were allowed to recover overnight. Next, a drug concentration range was added, and cell viability was determined 72 h later using 3-(4,5- dimethylthiazol-2-yl)-2,5-diphenyltetrazolium bromide (MTT at 5 mg/ml) as a substrate. Following a 5 h incubation period, formazan was solubilized with dimethylsulfoxide, and the absorbance was measured at 560 nm. Untreated cells served as a reference for 100 % cell viability.

2.4 In vivo orthotopic neuroblastoma studies

Animal studies were performed in accordance with the approved institutional protocol 13-166 of the Institutional Animal Care and Use Committee of Tufts University. All procedures were performed on female NCr nude mice (Taconic, Hudson, NY, USA) at 7 weeks of age. Procedures and ultrasound measurements were performed under general anesthesia using isoflurane inhalation. At least three animals were used for each experimental group, unless otherwise stated.

A transverse incision was made on the left flank. The abdominal viscera were retracted and the retroperitoneal space was entered. The left adrenal gland was located, and 2 μl of PBS containing

1×10^6 KELLY cells were injected into the adrenal gland via a 30G needle. When the tumor volume reached 70 mm^3, the animals were randomized and treated with 50 μg of doxorubicin incorporated into: (i) instantly soluble silk films; (ii) stabilized silk films; or (iii) stabilized silk films with a gold backing. The doxorubicin-containing silk surface was placed on the tumor and then the fascia and skin were closed in separate layers. The control groups consisted of stabilized silk film, and tail vein bolus injection of 50 μg doxorubicin in 100 μl of saline solution. An analogous protocol to the doxorubicin study was used for *in vivo* testing of soluble and stabilized silk films with a nominal crizotinib loading of 160 μg. Tumor volume was measured twice a week via ultrasound (detailed below) and animals were euthanized when the tumor volume exceeded 1,000 mm^3.

2.5 High Frequency Ultrasound measurements

The mouse was secured to the stage in a prone position. Next, a VisualSonics Vevo 2100 Sonographic probe (Toronto, Ontario, Canada) was applied to the left flank to locate the left adrenal gland and the tumor. Serial cross-sectional images (0.076 mm between images) were taken and the tumor volume was measured using the 3-D reconstruction tool (Vevo Software v1.6.0).

2.6 Statistical analysis

Data were analyzed using GraphPad Instat 5.0b (GraphPad Software, La Jolla, USA). Sample pairs were analyzed with the Student's t-test. Multiple samples were evaluated by one-way analysis of variance (ANOVA), followed by Bonferroni or Dunnett's post hoc tests to evaluate

the statistical differences ($P \leq 0.05$) among all samples or between samples and controls, respectively. All error bars represent standard deviations (s.d.).

3. RESULTS

All stabilized silk films conformed well to a tumor phantom, although the best fit was observed for the 1 %w/v films (Fig. 1a). Soluble silk films showed an excellent conformity that was independent of the silk content. A significant increase in mass was noted for the 2 and 4 %w/v silk films, but negligible increases in thickness (Fig. 1b). Only 1 %w/v films showed a significant increase in thickness but no significant change in weight. The swelling behavior was minimal for all films (Supplementary Fig. 1). Doxorubicin release from silk films was dependent on the amount of silk: 4 %w/v films showed a substantially slower release over the first 15 days when compared to 1 and 2 %w/v films (Fig. 1c). However, all films were able to release > 65 % of the loaded doxorubicin over 4 weeks. The gold backing significantly reduced the cumulative amount of doxorubicin released over 4 weeks (Fig. 1d); the slowest release kinetics were observed for 4 %w/v silk films and substantially faster release, albeit with similar kinetics, were observed for 1 and 2 %w/v films (Supplementary Fig. 2). Doxorubicin-loaded, gold-backed, soluble silk films (Fig. 1e) were compared to doxorubicin-loaded soluble silk films in an agar assay. The gold backing served as an effective barrier because it was able to modify doxorubicin release (Fig. 1d), and to restrict drug release from a bidirectional to a unidirectional release pattern (Fig. 1f).

Doxorubicin-loaded silk films were assessed *in vitro* for their ability to inhibit tumor growth over a two week period (Fig. 2 a). Soluble and stabilized silk control films did not significantly

change cell viability, but doxorubicin-loaded films reduced cell viability to < 6 % of the control. Similar results were observed for diffusible doxorubicin controls at the equivalent doxorubicin dose. However, only stabilized, doxorubicin-loaded silk films were able to control KELLY cell growth over the entire 15 days of the simulated disease relapse assay (Fig. 2a). None of the other doxorubicin-based treatment regimes controlled cell growth. Reseeding during the assay was preformed at day 6. This time point was selected because drug release from stabilized films continued at doses for at least another 5 days which affected KELLY growth.

In vivo neuroblastoma studies showed that doxorubicin treatment reduced tumor growth, with a similar response seen with 2 %w/v stabilized silk films in the presence and absence of a gold backing (Fig. 2b, c). Drug-loaded soluble silk films showed the best clinical response, while intravenous doxorubicin and stabilized 4 %w/v films showed similar *in vivo* responses (Fig. 2b, c). However, intravenous dosing of an equivalent doxorubicin dose was more effective than using 4 %w/v stabilized silk films with a gold backing and loaded with doxorubicin (Fig. 2b, c). The stabilized silk films were removed at the end of the *in vivo* study, and the amounts of doxorubicin retained in these films were quantified (Fig. 2d). Overall, significantly more drug remained in the 4 %w/v films when compared to the 2 %w/v films (Fig. 2d). The presence of a gold backing on either the 2 or 4 %w/v films resulted in greater retention of doxorubicin in the films when compared to respective films without the gold backing.

The silk films were also assessed for their ability to delivery the ALK targeted drug, crizotinib. Studies of the crizotinib loading capacity of silk films revealed that increasing the silk content from 1 to 4 %w/v significantly increased drug loading (Fig. 3a). Films were able to retain 29, 35,

and 57 % of the drug in 1, 2, and 4 %w/v films, respectively. Over the first 10 days, all films delivered comparable amounts of crizotinib so that release appeared to be independent of the amount of silk present in the film (Fig. 3b). The release from 1 %w/v films was exhausted from day 10 onwards while 2 and 4 %w/v films continued to release crizotinib for up to 20 days (Fig. 3b). Overall, significantly greater amounts of crizotinib were released from the 4 %w/v films than from the 1 %w/v films (Fig. 3b). Importantly, the release relative to crizotinib loading showed similar release profiles across all samples but with the lowest percentage release from 4 %w/v films (Supplementary Fig. 3).

The biological response of crizotinib-loaded silk films was also tested *in vitro* (Fig. 3c, Supplementary Fig. 4). Cytotoxicity studies with diffusible crizotinib showed that the IC_{50}s for KELLY and SK-N-AS cells were 1×10^4 nM and 7.5×10^3 nM, respectively (Supplementary Fig. 3). Cells were exposed to soluble and stabilized silk films loaded with crizotinib and compared with cells exposed to diffusible drug and soluble and stabilized control films (Fig. 3c). The SK-N-AS cells showed identical biological responses to diffusible crizotinib and stabilized silk films loaded with crizotinib for the first 6 days of the assay, with a reduction in cell viability to < 5 %, while soluble films loaded with crizotinib showed a reduction in cell viability to < 35 %. However, simulated relapse indicated that only the stabilized silk films loaded with crizotinib were able to inhibit cell proliferation (Fig. 3c). The *in vitro* response of KELLY cells showed a similar profile to that observed for SK-N-AS cells, whereby only stabilized silk films loaded with crizotinib were able to inhibit cell proliferation (Fig. 3c). A noticeable difference from the SK-N-AS cells was that the group treated with soluble silk films loaded with crizotinib and the diffusible crizotinib control group showed identical *in vitro* responses (Fig. 3c).

The *in vivo* response to stabilized silk films loaded with crizotinib was assessed in mice with orthotopic KELLY cell tumor (MYCN positive, ALK amplified) neuroblastomas. Crizotinib treatment slowed KELLY tumor growth and extended overall mouse survival by 3 days when compared to control films (Fig. 4).

4. DISCUSSION

Current methods for treatment of high-risk neuroblastoma patients include surgical intervention in addition to systemic chemotherapy that entails induction, consolidation, and maintenance phases [1, 2] for reducing the tumor burden. Nevertheless, the therapeutic tools available to pediatric surgeons involved in neuroblastoma care are limited. New options for the improved control of the site and kinetics of drug delivery would therefore have a major impact on treatment outcomes. The development of drug delivery systems for intraoperative use that can deliver a range of different therapeutic agents (e.g., chemotherapy, kinase inhibitors) would represent an important step towards improved patient care.

Here, we examined silk films for the focal therapy of neuroblastoma and present an entirely new approach for the treatment of unresectable neuroblastoma. Besides silk's ability to bind and release drugs [26], numerous biocompatibility studies have demonstrated that silk films are well tolerated *in vivo,* with minimal inflammation or host immune responses when implanted subcutaneously or directly into tissues (e.g., muscle, abdominal wall) [27-29]. The local tissue response is often significantly better than that seen with other FDA approved synthetic and degradable polymers (e.g., poly(lactic-co-glycolic acid) copolymers, polycaprolactone) or with

collagen [30]. The silk films developed here caused little swelling and conformed to tumor phantoms (Fig. 1a). We also showed that these films bind and release doxorubicin; a cytotoxic agent currently used for the treatment of neuroblastoma.

We and others have shown that silk is a useful biopolymer for drug delivery [18, 30]. Similar to previous observations with silk hydrogels [19], films with the highest silk content showed the slowest drug release kinetics when compared to films with lower silk content. However, there was no significant difference in drug release between the 1 %w/v and the 2% w/v films (Fig. 1c). We further refined our doxorubicin-loaded silk films by adding a gold backing. This gold nanolayer promoted a monodirectional drug release, as verified by agar assays (Fig. 1f). The overall effect of the gold backing was to maximize doxorubicin release towards the tumor while minimizing drug release into adjacent tissues. The gold backing provides a physical barrier to drug release; this concept is typically used in the design of transdermal patches [24].

We also examined the ability of doxorubicin-loaded silk films to inhibit the *in vitro* growth of KELLY neuroblastoma cells. The *in vitro* relapse assay showed that stabilized silk films outperformed all other delivery strategies and provided the best antitumor control (Fig. 2a). We therefore tested doxorubicin-loaded silk films *in vivo* using the orthotopic KELLY neuroblastoma tumor model. Overall, delivery of doxorubicin using 2 %w/v stabilized silk films or soluble silk films gave the best *in vivo* response (Fig. 1b), and this response could be further enhanced by resecting the tumor [31]. Changing the delivery route from intravenous dosing to local application would be expected to improve the side effect profile, particularly by reducing cardiotoxicity, which is currently a dose-limiting side effect in the clinic.

In the current study, we used a total cumulative doxorubicin dose of 50 μg, which was selected to maximize the antitumor effects in response to changed routes of administration. This dose is below the cumulative doxorubicin amount required to induced cardiotoxicity in an experimental rodent model [32]. Therefore, we were not able to provide definitive proof that changing doxorubicin administration from an intravenous bolus to focal therapy would reduce cardiotoxicity. We examined the amount of doxorubicin remaining in the films at the end of the *in vivo* study and found a good overall correlation between *in vitro* release studies—where gold-backed films retained more doxorubicin—and the results obtained *in vivo* (Fig. 1d, Fig. 2s, Supplementary Fig. 2).

Cytotoxic chemotherapy is an integral part of neuroblastoma care. Stratifying the patient population according to the molecular characteristics of the disease enables use of targeted therapies such as crizotinib. Here, we have selected the first generation ALK inhibitor, crizotinib, which is currently undergoing testing in neuroblastoma patients in Phase II clinical trials [33]. We anticipate that changing the route of administration from oral dosing to a localized application would have the potential benefits of reduced side effects and higher tissue concentration of the drug. For this reason, we examined the ability of silk to bind and release crizotinib.

The silk films were able to bind crizotinib similarly to doxorubicin, again in amounts that depended on the amount of silk present in each film (i.e., a significantly greater amount of drug was adsorbed to films with higher silk content) (Fig. 3a). Like doxorubicin, which has a logD of

1.12 at pH 7.4 and logD of 0.02 at pH 5.5, crizotinib is a weak base with logD value of 2.25 at pH 7.4 and a logD value of 0.74 at pH 5.5. Structure/activity relationships of model drugs have shown that weakly basic, small molecular weight compounds exhibit binding and release kinetics that are dependent on logD [34, 35]. We therefore predicted that crizotinib would also be loaded into silk films through adsorption: (i) by interacting with the hydrophobic silk domains and (ii) by charge-charge interactions of the weakly basic drug with the negative net charge of silk.

The total loading of crizotinib was significantly greater for the 4 %w/v films than for the 1 %w/v films and the loaded drug was released for up to 30 days in the films with higher silk content (Fig. 3a). Crizotinib release was monitored by (i) determining the amount of drug release (Fig. 3b), and (ii) correcting for differences in loading and expressing the data as percentage release of total (Supplementary Fig. 3). The latter release kinetics were similar to doxorubicin release seen here (Fig. 1c) and previously for silk hydrogels [26]; here we show that 4 %w/v films were able to retain crizotinib substantially better than 1 and 2 %w/v films. Our *in vitro* neuroblastoma relapse assay confirmed that the stabilized silk films loaded with crizotinib outperformed all other drug delivery strategies. As might be predicted from the ALK status, KELLY cells showed a better response to treatment than did SK-N-AS cells.

We then examined the *in vivo* response of orthotopic KELLY tumors in mice treated with crizotinib-loaded silk films. These studies did not include the oral dosing of mice with crizotinib because a pilot study indicated a substantial weight loss in mice subjected to oral dosing (> 15 % of body weight) during the first 3 days of the study. This necessitated the exclusion of this treatment group from our study. We observed some antitumor activity with stabilized silk films

loaded with crizotinib in these preliminary *in vivo* studies; however, further refinements in the crizotinib-loaded films are still needed to test drug release kinetics (e.g., instant, intermediate, slow), drug loading (e.g., dose escalation), and tumor resection followed by film application, in order to more closely mimic the clinical scenario.

5. CONCLUSION

We successfully manufactured silk films for neuroblastoma care that can be: (i) readily loaded with a cytotoxic and targeted drug; (ii) fine tuned to achieve drug release kinetics that range from instantaneous release (i.e., minutes) to prolonged release (28 days); and (iii) easily placed directly onto the tumor to achieve good conformity and subsequent focal therapy. Both *in vitro* and *in vivo* studies indicated that drug-loaded silk films showed improved antitumor efficacy when compared to the current route of drug administration.

ACKNOWLEDGMENTS

The authors would like to thank Dr. David J. Wilbur of Tufts University, Department of Chemistry for technical assistance with the LC-MS. The NSF grant #CHE-0320783 supports the Tufts University Analytical and Mass Spectrometry Core Facility. The project described was supported by NIH grant P41 EB002520-05 (Tissue Engineering Resource Center) (DLK), a Mildred Scheel Postdoctoral fellowship from the German Cancer Aid (FPS), a Marie Curie FP7 Career Integration Grant 334134 within the 7th European Union Framework Program (FPS), the National Center for Advancing Translational Sciences, Tissue Engineering Resource Centre National Institutes of Health, Grant Numbers UL1 TR000073, UL1 TR001064, and P41 EB002520.

DISCLOSURE STATEMENT

The authors have no competing financial interests.

REFERENCES

[1] Maris JM. Recent advances in neuroblastoma. N Engl J Med 2010;362:2202-11.

[2] Hara J. Development of treatment strategies for advanced neuroblastoma. Int J Clin Oncol 2012;17:196-203.

[3] Warmann SW, Seitz G, Schaefer JF, Scheel-Walter HG, Leuschner I, Fuchs J. Vascular encasement as element of risk stratification in abdominal neuroblastoma. Surg Oncol 2011;20:231-5.

[4] Carpenter EL, Mosse YP. Targeting ALK in neuroblastoma--preclinical and clinical advancements. Nat Rev Clin Oncol 2012;9:391-9.

[5] Chen Y, Takita J, Choi YL, Kato M, Ohira M, Sanada M, et al. Oncogenic mutations of ALK kinase in neuroblastoma. Nature 2008;455:971-4.

[6] George RE, Sanda T, Hanna M, Frohling S, Luther W, 2nd, Zhang J, et al. Activating mutations in ALK provide a therapeutic target in neuroblastoma. Nature 2008;455:975-8.

[7] La Quaglia MP, Kushner BH, Su W, Heller G, Kramer K, Abramson S, et al. The impact of gross total resection on local control and survival in high-risk neuroblastoma. J Pediatr Surg 2004;39:412-7; discussion -7.

[8] Hanahan D, Weinberg RA. Hallmarks of cancer: the next generation. Cell 2011;144:646-74.

[9] Duncan R, Gaspar R. Nanomedicine(s) under the microscope. Mol Pharm 2011;8:2101-41.

[10] de Melo-Diogo D, Gaspar VM, Costa EC, Moreira AF, Oppolzer D, Gallardo E, et al. Combinatorial delivery of Crizotinib-Palbociclib-Sildenafil using TPGS-PLA micelles for improved cancer treatment. Eur J Pharm Biopharm 2014;88:718-29.

[11] Marques JG, Gaspar VM, Markl D, Costa EC, Gallardo E, Correia IJ. Co-delivery of Sildenafil (Viagra((R))) and Crizotinib for synergistic and improved anti-tumoral therapy. Pharm Res 2014;31:2516-28.

[12] Pastorino F, Brignole C, Loi M, Di Paolo D, Di Fiore A, Perri P, et al. Nanocarrier-mediated targeting of tumor and tumor vascular cells improves uptake and penetration of drugs into neuroblastoma. Front Oncol 2013;3:190.

[13] Veronesi U, Cascinelli N, Mariani L, Greco M, Saccozzi R, Luini A, et al. Twenty-year follow-up of a randomized study comparing breast-conserving surgery with radical mastectomy for early breast cancer. N Engl J Med 2002;347:1227-32.

[14] Brem H, Piantadosi S, Burger PC, Walker M, Selker R, Vick NA, et al. Placebo-controlled trial of safety and efficacy of intraoperative controlled delivery by biodegradable polymers of chemotherapy for recurrent gliomas. The Polymer-brain Tumor Treatment Group. Lancet 1995;345:1008-12.

[15] Westphal M, Ram Z, Riddle V, Hilt D, Bortey E, Executive Committee of the Gliadel Study G. Gliadel wafer in initial surgery for malignant glioma: long-term follow-up of a multicenter controlled trial. Acta Neurochir (Wien) 2006;148:269-75; discussion 75.

[16] Omenetto FG, Kaplan DL. New opportunities for an ancient material. Science 2010;329:528-31.

[17] Vollrath F, Porter D. Silks as ancient models for modern polymers. Polymer 2009;50:5623-32.

[18] Seib FP, Kaplan DL. Silk for Drug Delivery Applications: Opportunities and Challenges. Israel Journal of Chemistry 2013;53:756-66.

[19] Seib FP, Pritchard EM, Kaplan DL. Self-assembling doxorubicin silk hydrogels for the focal treatment of primary breast cancer. Adv Funct Mater 2013;23:58-65.

[20] Seib FP, Jones GT, Rnjak-Kovacina J, Lin YN, Kaplan DL. pH-Dependent Anticancer Drug Release from Silk Nanoparticles. Advanced Healthcare Materials 2013;2:1606-11.

[21] Kim DH, Viventi J, Amsden JJ, Xiao J, Vigeland L, Kim YS, et al. Dissolvable films of silk fibroin for ultrathin conformal bio-integrated electronics. Nat Mater 2010;9:511-7.

[22] Kim RH, Kim DH, Xiao J, Kim BH, Park SI, Panilaitis B, et al. Waterproof AlInGaP optoelectronics on stretchable substrates with applications in biomedicine and robotics. Nat Mater 2010;9:929-37.

[23] Cirillo B, Morra M, Catapano G. Adhesion and function of rat liver cells adherent to silk fibroin/collagen blend films. Int J Artif Organs 2004;27:60-8.

[24] Kearney CJ, Mooney DJ. Macroscale delivery systems for molecular and cellular payloads. Nat Mater 2013;12:1004-17.

[25] Rockwood DN, Preda RC, Yucel T, Wang X, Lovett ML, Kaplan DL. Materials fabrication from Bombyx mori silk fibroin. Nat Protoc 2011;6:1612-31.

[26] Seib FP, Kaplan DL. Doxorubicin-loaded silk films: drug-silk interactions and in vivo performance in human orthotopic breast cancer. Biomaterials 2012;33:8442-50.

[27] Ma X, Cao C, Zhu H. The biocompatibility of silk fibroin films containing sulfonated silk fibroin. J Biomed Mater Res B Appl Biomater 2006;78:89-96.

[28] Meinel L, Hofmann S, Karageorgiou V, Kirker-Head C, McCool J, Gronowicz G, et al. The inflammatory responses to silk films in vitro and in vivo. Biomaterials 2005;26:147-55.

[29] Panilaitis B, Altman GH, Chen J, Jin HJ, Karageorgiou V, Kaplan DL. Macrophage responses to silk. Biomaterials 2003;24:3079-85.

[30] Yucel T, Lovett ML, Kaplan DL. Silk-based biomaterials for sustained drug delivery. J Control Release 2014.

[31] Chiu B, Coburn J, Pilichowska M, Holcroft C, Seib FP, Charest A, et al. Surgery combined with controlled-release doxorubicin silk films as a treatment strategy in an orthotopic neuroblastoma mouse model. Br J Cancer 2014.

[32] Doroshow JH, Locker GY, Ifrim I, Myers CE. Prevention of doxorubicin cardiac toxicity in the mouse by N-acetylcysteine. J Clin Invest 1981;68:1053-64.

[33] Matthay KK, George RE, Yu AL. Promising therapeutic targets in neuroblastoma. Clin Cancer Res 2012;18:2740-53.

[34] Lammel A, Schwab M, Hofer M, Winter G, Scheibel T. Recombinant spider silk particles as drug delivery vehicles. Biomaterials 2011;32:2233-40.

[35] Hines DJ, Kaplan DL. Mechanisms of controlled release from silk fibroin films. Biomacromolecules 2011;12:804-12.

FIGURE LEGENDS

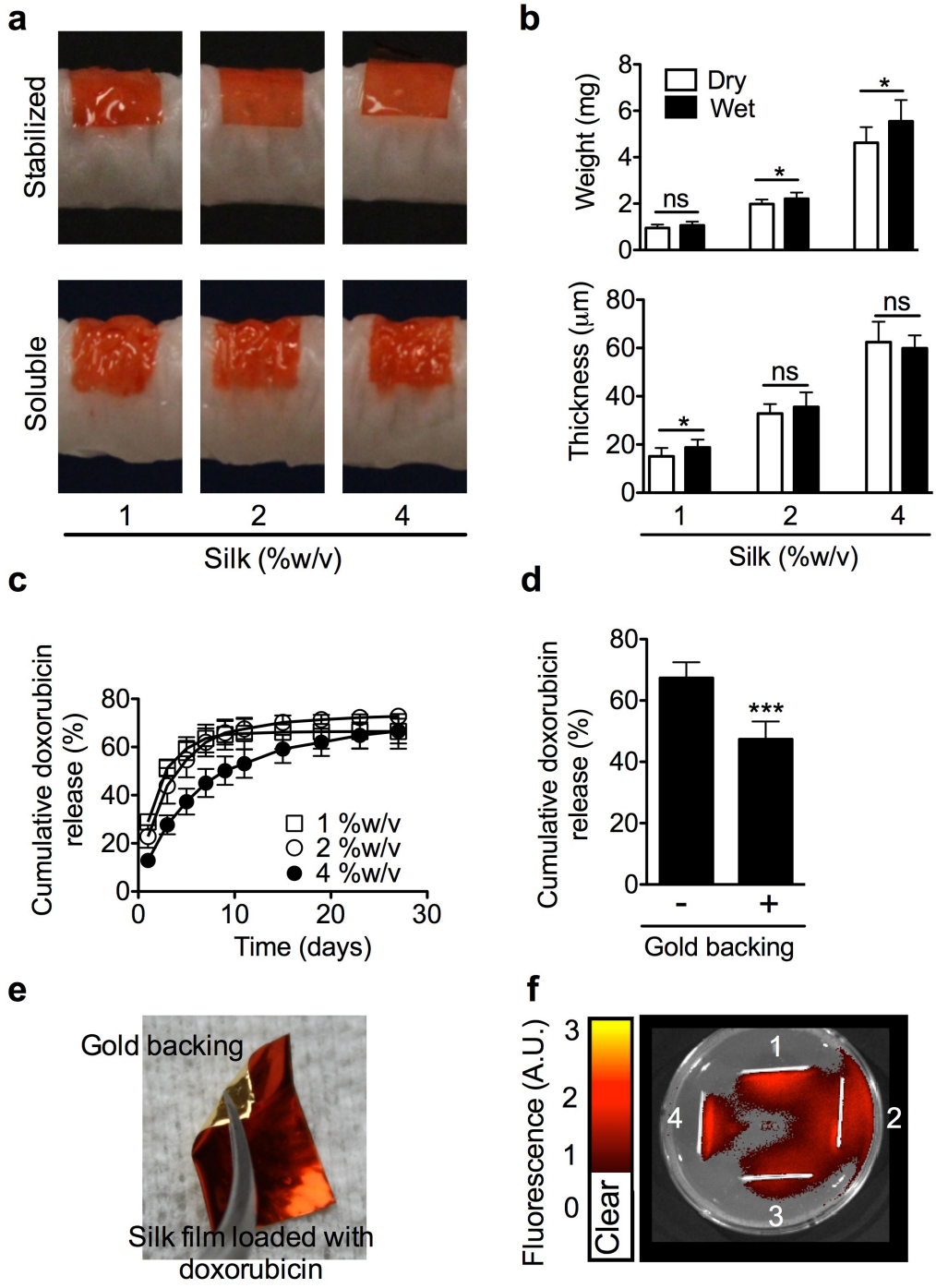

Figure 1. Characterization of silk films intended for local neuroblastoma therapy. (**a**) Conformity of silk films to tumor phantoms; (**b**) Weight and thickness of silk films in the dry and hydrated state; (**c**) Doxorubicin release kinetics from stabilized silk films; (**d**) Cumulative doxorubicin

release from 4 %w/v silk films in the presence and absence of a gold backing; (**e**) An example of a doxorubicin-loaded silk film with a gold backing; (**f**) Doxorubicin release into a three dimensional agarose gel in the presence (1 and 4) and absence (2 and 3) of gold backing. (Error bars, s.d.; ***$P < 0.001$; $n \geq 3$)

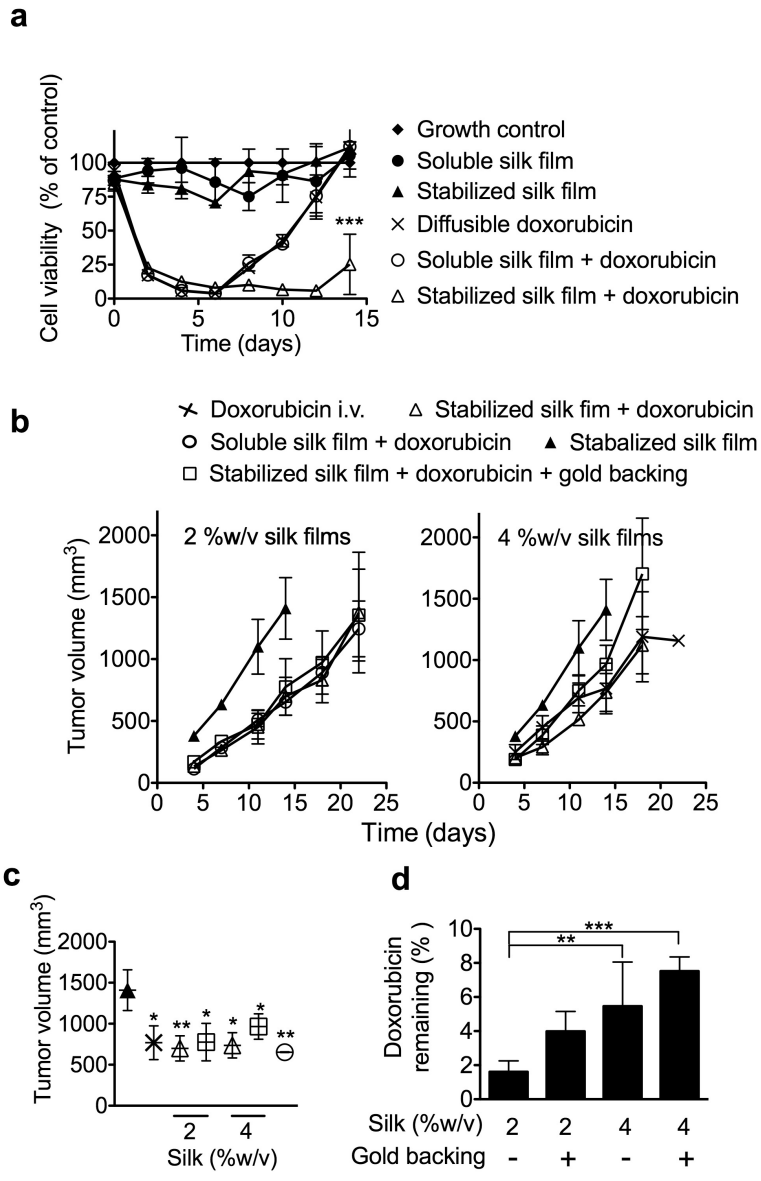

Figure 2. *In vitro* and *in vivo* response of doxorubicin-loaded silk films. (a) Long term toxicity of free doxorubicin and silk films loaded with doxorubicin. Culture medium was replaced at the indicated time. With the exception of control wells, wells were re-seeded with the cells at day 6. (**b**) Treatment response of orthotopic KELLY neuroblastomas, (**c**) tumor volume at the end of the *in vivo* study. (**d**) Quantification of the amount of doxorubicin remaining in stabilized silk films at the end of the *in vivo* study. (Error bars, s.d.; $^{**}P < 0.005$, $^{***}P < 0.001$; $n \geq 3$)

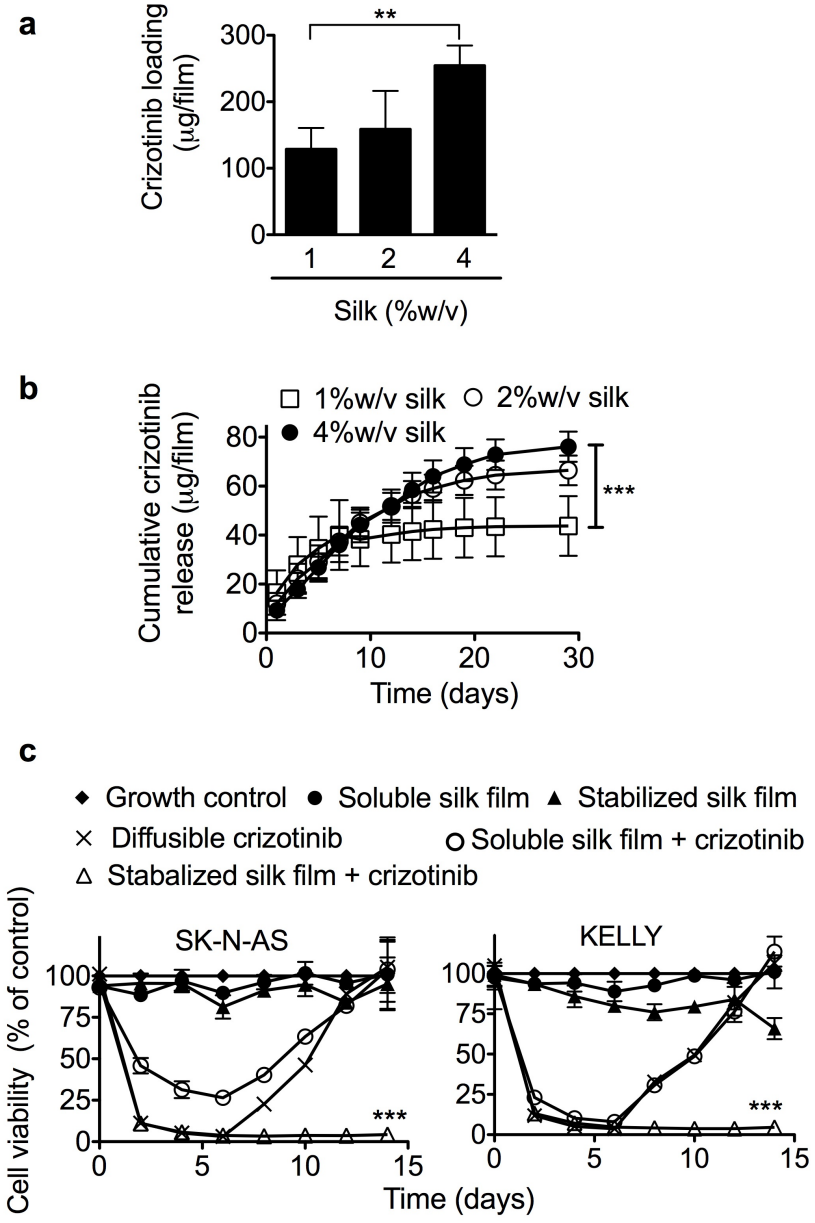

Figure 3. Characterization of crizotinib-loaded silk films. (**a**) Loading capacity of stabilized silk films: films were loaded with crizotinib by drug adsorption from solution. (**b**) Cumulative crizotinib release from silk films. (**c**) Long term *in vitro* response of SK-N-AS and KELLY (ALK amplified) cells to crizotinib-loaded silk films and controls; films were generated using 2 %w/v

silk. Culture medium was replaced at the indicated time. With the exception of control wells, wells were re-seeded with the cells at day 6. (Error bars, s.d.; $^{**}P < 0.005$, $^{***}P < 0.001$; n ≥ 3)

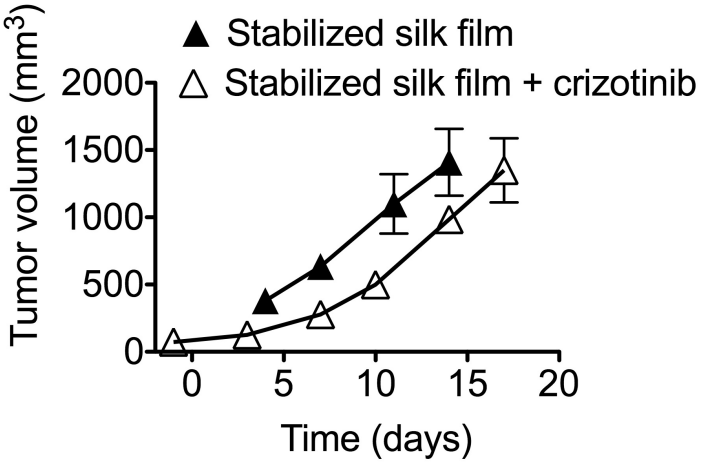

Figure 4. *In vivo* response of orthotopic KELLY neuroblastoma tumors treated with crizotinib-loaded silk films. Comparison of stabilized silk films ± crizotinib. (Error bars, s.d.; n ≥ 3)

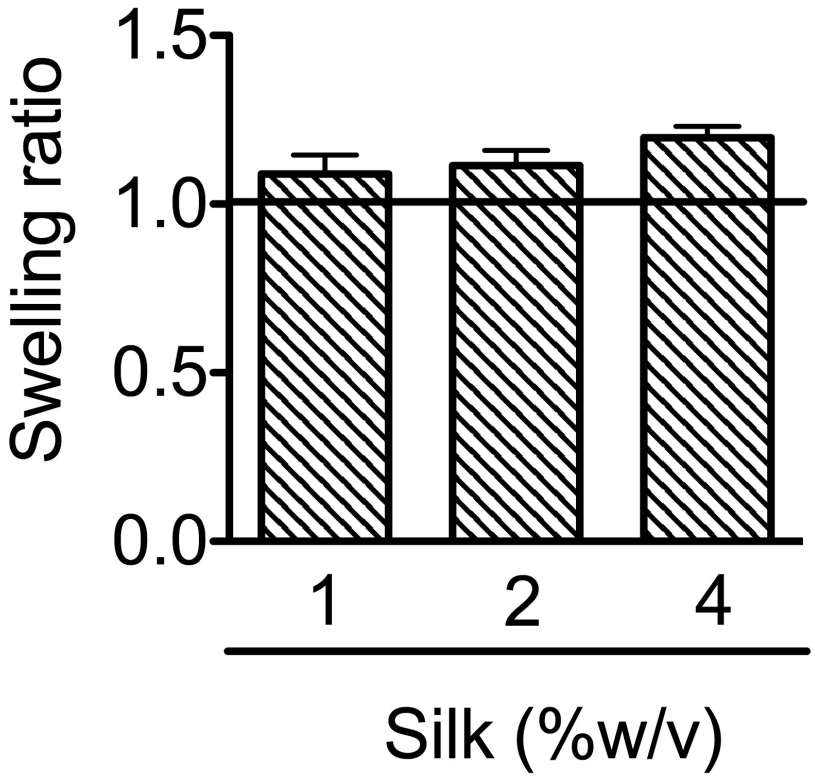

Supplementary Figure 1. Swelling behavior of stabilized silk films in phosphate buffered saline. (Error bars, s.d.; n ≥ 3)

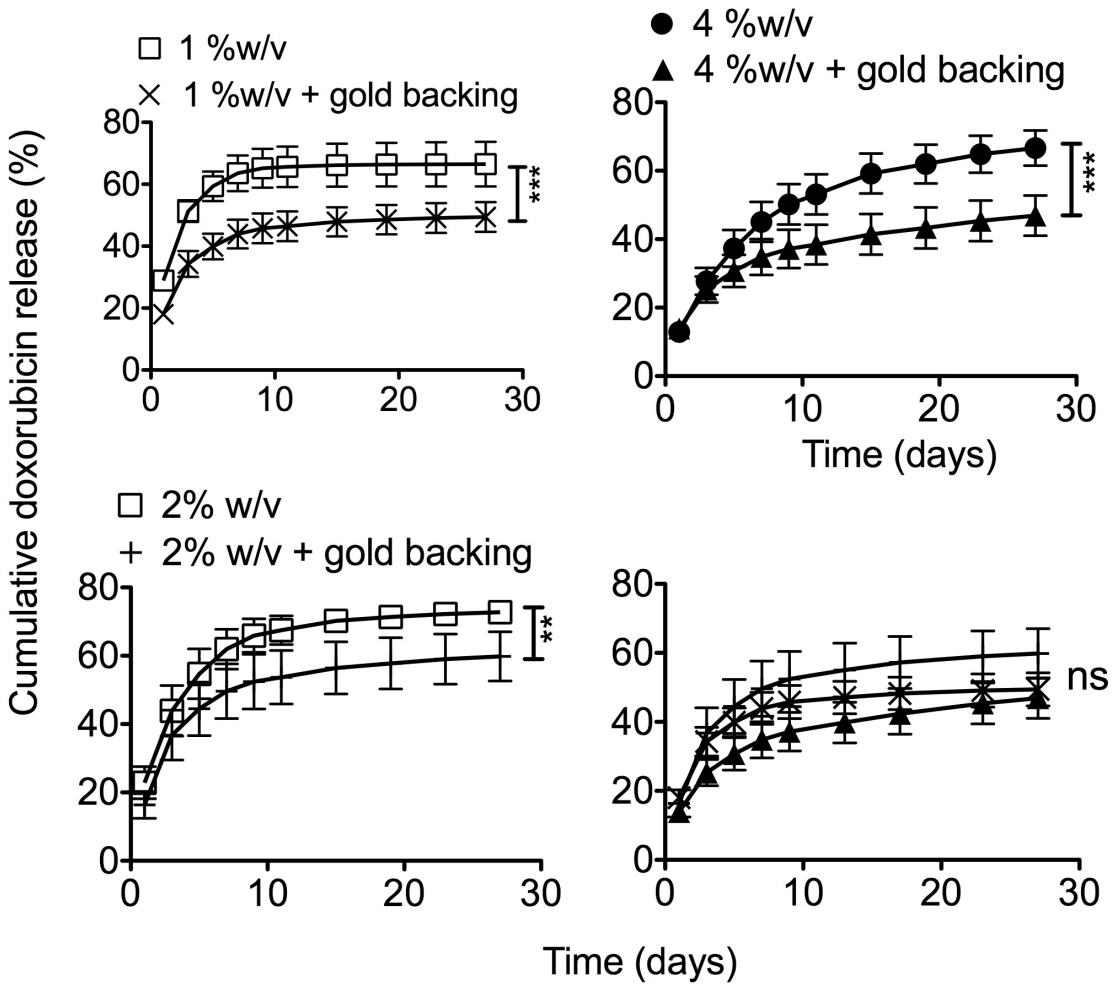

Supplementary Figure 2. Cumulative doxorubicin release kinetics from stabilized silk films in the presence and absence of a gold backing. (Error bars, s.d.; $n \geq 3$)

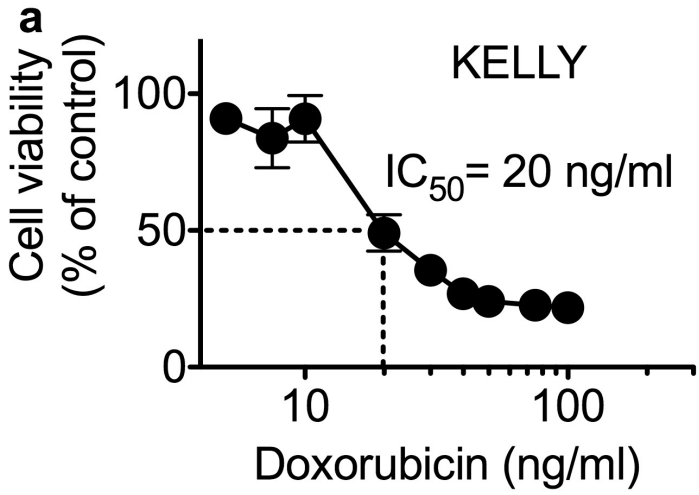
a
KELLY
Cell viability (% of control)
100
50
0
IC50= 20 ng/ml
10
100
Doxorubicin (ng/ml)

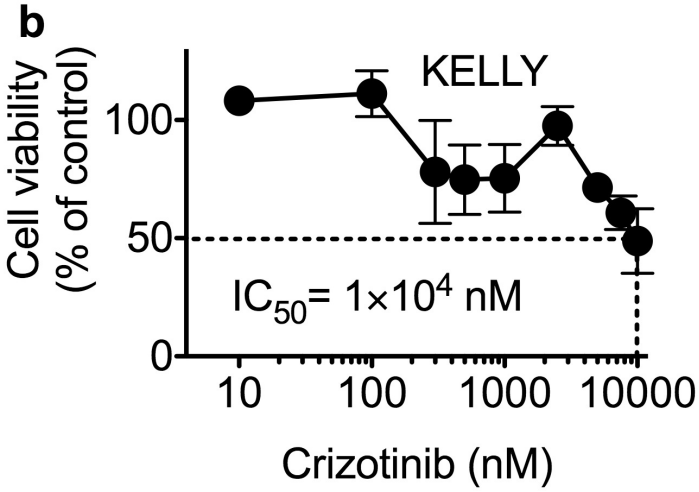
b
KELLY
Cell viability (% of control)
100
50
0
IC50= 1×10^4 nM
10
100
1000
10000
Crizotinib (nM)

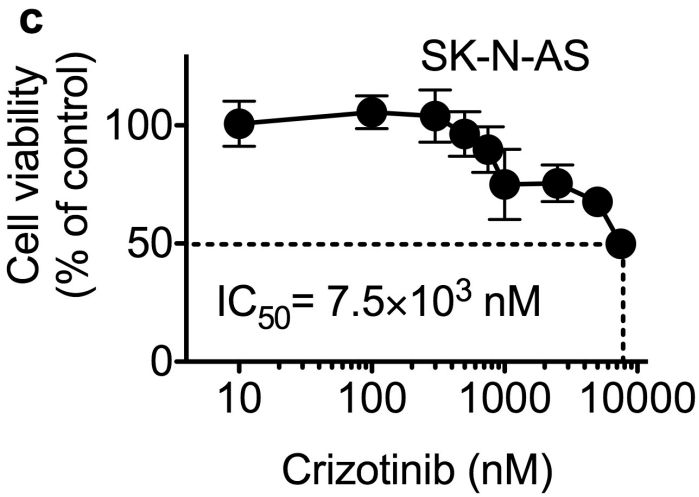
c
SK-N-AS
Cell viability (% of control)
100
50
0
IC50= 7.5×10^3 nM
10
100
1000
10000
Crizotinib (nM)

Supplementary Figure 3. Cumulative crizotinib release from stabilized silk films. (Error bars, s.d.; n ≥ 3)

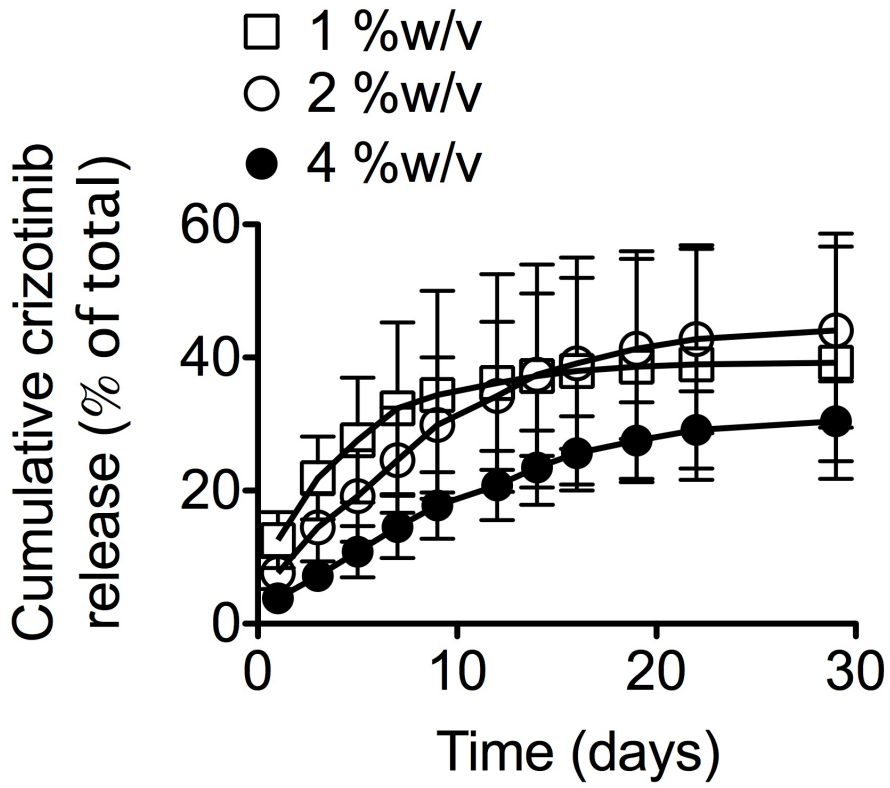

Supplementary Figure 4. Cytotoxicity and respective IC_{50}s for SK-N-AS and KELLY cells treated with diffusible crizotinib. (Error bars, s.d.; n ≥ 3)